Anal. Bioanal. Electrochem., Vol. 12, No. 1, 2020, 107-127

Analytical & Bioanalytical Electrochemistry

2020 by CEE
www.abechem.com

Review

Effect of Grain Refinement on the Semiconducting Behaviors of Passive Films Formed on Pure Copper: A Review

Arash Fattah-alhosseini,* Omid Imantalab and Kazem Babaei

Department of Materials Engineering, Bu-Ali Sina University, Hamedan 65178-38695, Iran

*Corresponding Author, Tel.: +988138292505; Fax: +988138257400

E-Mail: a.fattah@basu.ac.ir

Received: 19 November 2019 / Accepted with minor revision: 5 January 2020 / Published online: 31 January 2020

Abstract- Materials of ultrafine–grained (UFG) have attracted great attention in the last twenty years. Some severe plastic deformation (SPD) procedures have been utilized for producing UFG materials in which the accumulative roll bonding (ARB) process acts as the most effective procedure among them. UFG Structure demonstrates a progress in mechanical properties in addition to different corrosion behavior. Nevertheless, it does not always lead to better corrosion resistance. Various relevant investigations will be reviewed in this paper to consider semiconducting behavior of UFG Cu that has been produced by ARB process. Analysis of Mott–Schottky (M–S) is a major in-situ method to analyze semiconductor properties of passive layers. Thus, the effect of grain size arising from ARB process on copper semiconducting behavior has been evaluated in relevant passive media by M–S analysis in this study.

Keywords- Pure copper, Grain refinement, Semiconducting behavior, Passive film, Mott–Schottky (M–S) analysis

---

1. INTRODUCTION

Protection against corrosion of some metals and alloys is created by the passive films growth in aqueous solutions. This surface behavior is necessary to make sustainable developments in many usages and industries where metallic constituents are utilized. Passive films do not mainly exceed a few nanometers of thickness at ambient temperature [1,2]. Passive

films are excellent adherent and effectively separate the substrate from the aggressive environment. However, in the existence of aggressive species, passive films are sensitive to localized corrosion [3–6]. The passive current density of many reactive transition metals such as Ni, Fe, Cr and their alloys that are faced with aqueous ambiences is of the order ~0.01−1.0 $\mu A/cm^2$ [7]. The very complicated passivation phenomena can be influenced by several factors such as composition of alloy, the formation conditions and the environment characteristics [8]. Oxide passive layers that were grown on surfaces of metal and alloy have been widely reviewed [1,9].

Copper is widely utilized in industrial uses, power generation, corrosion prevention and tubes of heat exchanger [10–14]. According to the Pourbaix diagram of Cu in water [15], at values of pH varying from 6.8 to 12.8 the surface layer produced on copper is protective [16]. The copper passive behavior is influenced by the concentration of hydroxide electrolytes that are common corrosive environments in many industrial procedures. Thus, there are great concerns and requirements in order to investigate the passivation of Cu within alkaline electrolytes in detail. There are some studies on the copper passive behavior in alkaline electrolytes that have studied the protective behavior of passive layers in addition to the electrochemical production of copper oxide films [17].

Although a lot of investigations have been reported the passive and corrosion behavior of Cu and its alloys, there is little knowledge about the affection of grain refinement on the semiconducting behavior of the formed oxide layer on the pure copper [18–27]. Diverse relevant work is reviewed in this paper in order to date the studied semiconducting behavior of UFG copper, having produced utilizing ARB procedure.

2. MOTT–SCHOTTKY (M–S) ANALYSIS

M–S analysis has been indicated to be a significant in-situ technique to study passive films semiconductor properties. This analysis has been highly utilized in order to investigate the passive films semiconducting behaviors including the passive layers on Ni and its alloys [28–35], Al [36–39], Ti [40–49], Ta [50–57], Mg alloys [58–64], Cr [65], Zn [66], W [56], Zr [67], carbon steels [68–70] and stainless steels [6,71–79]. Based on the point defect model [9,80–83], the defects are cation and oxygen vacancies, and cation interstitials in the passive layer. It is considered that vacancies of oxygen and cation interstitials are electron donors, leading to n-type doping when vacancies of cation are electron acceptors and as a result, doping the barrier film p-type. M–S measurement is a strong technique in order to measure the passive layers semiconductive properties on metals and their alloys [16,17,22,84–86]. M–S relations that are utilized in order to specify the dopant density and semiconductor type of the passive layers, are [4,5,75,87]:

$$\frac{1}{C^2}=\frac{2}{\varepsilon\varepsilon_0 e N_D}\left(E-E_{FB}-\frac{kT}{e}\right) \qquad \text{n-type behavior} \qquad (1)$$

$$\frac{1}{C^2}=-\frac{2}{\varepsilon\varepsilon_0 e N_A}\left(E-E_{FB}-\frac{kT}{e}\right) \qquad \text{p-type behavior} \qquad (2)$$

where N_D and N_A are the densities of donor and acceptor, ε is the passive film dielectric constant, ε_0 stands for the vacuum permittivity, k stands for the Boltzmann constant, and U_{FB} shows the flat-band potential [4,5,75,87].

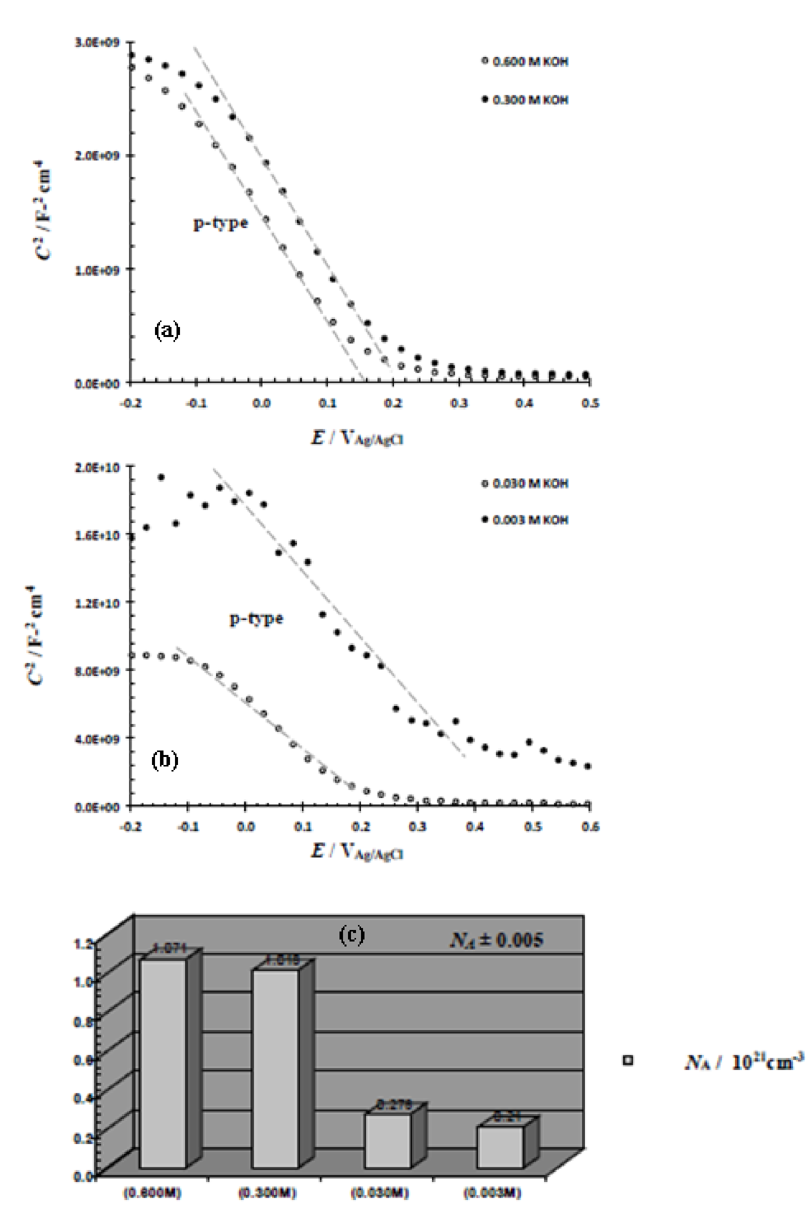

Fig. 1. (a, b) M–S plots and (c) variations in the N_A of pure Cu specimens in KOH solutions [10]

3. SEMICONDUCTING PROPERTIES OF PURE COPPER

Table 1 indicates the pure Cu semiconducting properties [10,11,88–93]. Fig. 1 shows the M–S plots and variations in the N_A of pure Cu specimens in KOH solutions [10]. It is obvious that capacitances apparently increase by rising the solutions concentration (Fig. 1(a) and (b)) [10].

Table 1. The semiconducting properties of pure copper

Solution	Semiconducting behavior	Year	First author [Ref]
0.2 M Boric acid buffer solution	The semiconductor character of passive film changed from p–type into n–type in the solution with high Cl^- concentration.	2011	Wang [88, 90]
Sulfide-containing aqueous solutions	The results indicate that a bi-layer sulfide film forms, comprising of a p-type barrier layer of Cu_2S and probably an outer layer of CuS, which is n-type in electronic character.	2013	Ling [89]
KOH Solutions (0.600, 0.300, 0.030 and 0.003 M KOH) at 25±1 ºC	In the M–S analysis, no evidence for n-type behavior was obtained. Also, M–S analysis revealed that with the decrease of solution concentration, the N_A of the passive films increased.	2015	Fattah-alhosseini [10]
NaOH solutions (0.050, 0.010, 0.005, and 0.001 M) at 25±1 ºC	In M–S analysis, no evidence of n-type semiconducting behavior was found. Also, M–S analysis indicated that with the decrease of NaOH concentration in the solution, the N_A of passive films increases.	2015	Fattah-alhosseini [11]
Anaerobic sulphide solutions	The passive film displayed p-type semiconductor behavior and the N_A (cation vacancy) was approximately 10^{22} to 10^{23} cm^{-3}.	2017	Kong [91]
0.0002 M $Na_2S{\cdot}9H_2O$+0.1 M NaCl	The whole passivation range shows p-type semiconductor characteristics and the magnitude of the acceptor density is 10^{23} cm^{-3}, which increases with increasing temperature.	2017	Kong [92]
0.1 M NaOH solutions with different chloride concentrations	P-type semiconducting characteristics were obtained with or without chloride. The density of copper vacancies was approximately 10^{20} cm^{-3}, and increased with the increasing chloride concentration, which was attributed to faster film formation in a higher chloride environment.	2018	Kong [93]

In addition, there is a zone in which E and C^{-2} have a somehow linear relationship in all of the M–S plots. The negative slope in this zone is ascribed to p-type semiconducting behavior because of the existence of Cu_2O in the passive layers. In general, passivity is because of the Cu_2O formation that is fairly stable within alkaline electrolytes. It has been depicted that there is a Cu oxide formation at open circuit potential as a passive film grows on Cu [11]. The orders

of magnitude of the N_A are about 10^{21} cm^{-3} and are comparable to those published in other research [11,91–93]. These high amounts of the N_A can be ascribed to the Cu vacancies higher density [10].

4. INFLUENCE OF GRAIN REFINEMENT ON THE SEMICONDUCTING PROPERTIES

Table 2 indicates how the grain refinement affects the semiconducting properties of pure Cu [94,95]. Fig. 2 depicts the schematic of ARB process used to obtain FG and UFG pure Cu [12]. More details about this process have been described [12–14,96]. Fig. 3(a) shows the pure Cu with annealed microstructure using optical microscope which divulges the mean grain size about 26 μm [97]. Transmission electron microscope (TEM) microstructures of ARB samples that were made by 3, 5 and 7 cycles are revealed as shown in Figs. 3(b)-(d) [96,97]. In the sample having 3 cycles, the microstructure got steady and grains having grain size average of nearly 200 nm were created. As illustrated in Fig. 3(c), having risen the strain to 5 cycles resulted in formation of little recrystallized grains that were seen with the ultra-fine deformation microstructures. These equiaxed recrystallized grains mean grain size is less than 120 nm and they are also finer than that for the sample having 3 passes. For the specimen having 7 cycles (Fig. 3(d)), these equiaxed recrystallized grains mean grain sizes are less than 80 nm and also finer than that of having 5 cycles. Rising strain up to 7 cycles also led the selected area diffraction (SAD) pattern to become more ring-like, indicating an increment in a part of the boundary with high angle [97].

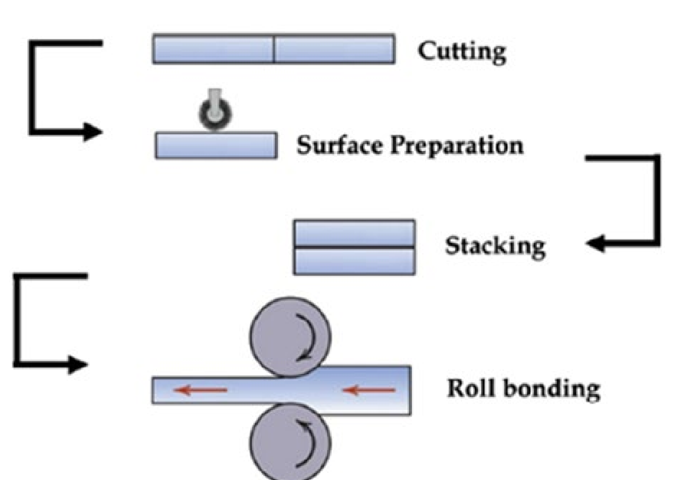

Fig. 2. Schematic illustration of the ARB process [12]. (With permission from Ref. [12]; License Number: 4707910404770, License date: Nov 14, 2019)

Table 2. The influence of grain refinement on the semiconducting properties of pure copper

Solution	Grain refinement process	Average Grain size	Semiconducting behavior	Year	First author [Ref]
Chromate solutions	ECAP process with up to 4 passes	~100 nm	Donor density (N_D) of the passive films formed on UFG Cu is higher than that of the passive films on coarse-grained Cu	2009	Wang [94]
Borate Buffer Solution (pH=8.4)	Annealing	~12 µm	With the decrease of the grain size, the acceptor density (N_A) of the passivation film on the surface of Cu was reducing	2013	Zhong [95]
0.01 M borax solution	ARB process with up to 8 passes	----	In M–S analysis, no evidence for n-type behavior was obtained. M–S analysis revealed that with increasing the number of ARB cycles, N_A of the passive films decreased.	2015	Fattah-alhosseini [12]
0.01 M borax solution (pH=9.1)	ARB process with up to 7 cycles	< 200 nm	M–S analysis showed that the increasing number of ARB cycles offer better conditions for forming the passive films with higher protection behavior, due to the growth of less-defective films	2015	Imantalab [13]
0.01 M KOH solution	ARB process with up to 6 cycles	----	M–S analysis revealed that with increasing the number of ARB cycles, the N_A of the passive films decreased	2015	Imantalab [14]
0.01 M borax solution (pH = 9.1)	Friction stir welding (FSW) process	----	According to M–S analysis, it was found that the N_A decreased with decreasing the grain size of the stir zone.	2016	Fattah-alhosseini [16]
Phosphate buffer solutions (pH ranging from 10.69 to 12.59)	ARB process	< 100 nm	M–S analysis indicated that the passive films behaved as p-type semiconductors and grain refinement did not change the semiconductor type of passive films.	2016	Imantalab [17]
0.01 M Borax solution	ARB process with up to 7 passes	< 120 nm	M–S analysis revealed that with increasing the number of ARB passes, the N_A of the passive films decreased	2016	Fattah-alhosseini [18]
phosphate buffer solution (pH =10.69)	ARB process with up to 4 cycles	~200 nm	M–S analysis showed that the electrochemical behavior improved by increasing the number of ARB cycle	2016	Imantalab [19]
0.01 M Borax solution	ARB process	< 100 nm	A superior behavior of NG sample in comparison to CG one was distinguished by its smaller cyclic	2016	Fattah-alhosseini [20]

(pH = 9.15)	with up to 8 passes		voltammogram loops, larger capacitive arcs in the Nyquist plots, and less charge carrier densities within the passive film.		
0.01 M KOH solution	ARB process with up to 8 passes	< 100 nm	M–S analysis showed that the surface films formed on annealed and NG samples in KOH solution with and without NaCl addition are of p-type semiconducting behavior. Moreover, M–S analysis showed that the N_A increases by increasing chloride ion concentration.	2016	Fattah-alhosseini [21]
0.01 M NaOH solution	cold deformation	----	In the M-S analysis, no evidence for n-type behavior was obtained. Also, M-S analysis revealed that with increasing cold deformation, the N_A of the passive films decreased.	2016	Fattah-alhosseini [22]
Borate buffer solution (pH=9.15)	ARB process with up to 4 passes	~200 nm	All electrochemical tests showed that the electrochemical behavior of pure copper is improved under influence of ARB process, mainly due to the formation of thicker and less defective oxide film.	2016	Fattah-alhosseini [23]
0.01 M KOH solution	ARB process with up to 8 passes	< 100 nm	It is speculated that high-quality passive layers relate to the presence of high-density structural defects on the surface of NG samples.	2017	Fattah-alhosseini [24]
Phosphate buffer solution (pH=10.69)	ECAP process with up to 6 passes	----	It is well found that the N_A of the passive film decreased with the increase of ECAP passes.	2017	Gholami [25]
0.1 M NaOH solution	ECAP process with up to 6 passes	~230 nm	M–S analysis indicates that although the passive film of ECAPed Cu still behaves as a p-type semiconductor, it becomes less defective or less conductive as the number of applied ECAP passes increase.	2018	Naseri [26]
0.1 M KOH solution	ARB process with up to 9 cycles	~80 nm	The findings clarify that the vacancy of copper is the main in the passive layer on both annealed and nano-grained pure copper formed anodically in 0.1 M KOH electrolyte.	2018	Fattah-alhosseini [27]

Figs. 4 and 5 show the M–S plots and variations in the N_A of pure Cu samples in 0.01 M borax [12] and 0.01 M KOH solutions [14], respectively. It is obvious that capacitances clearly rise by augmenting the cycles of ARB (Fig. 4(a) and Fig. 5(a)). Based on Fig. 4(b) and Fig. 5(b), the N_A declines with the number of ARB cycles. The changes in the N_A is related to the non-stoichiometry defects within the passive layers. The orders of magnitude of the N_A are

about 10^{20} cm^{-3} and are comparable to those published in other investigations [10,11]. These high amounts of the N_A can be ascribed to the Cu vacancies higher density in the passive layers.

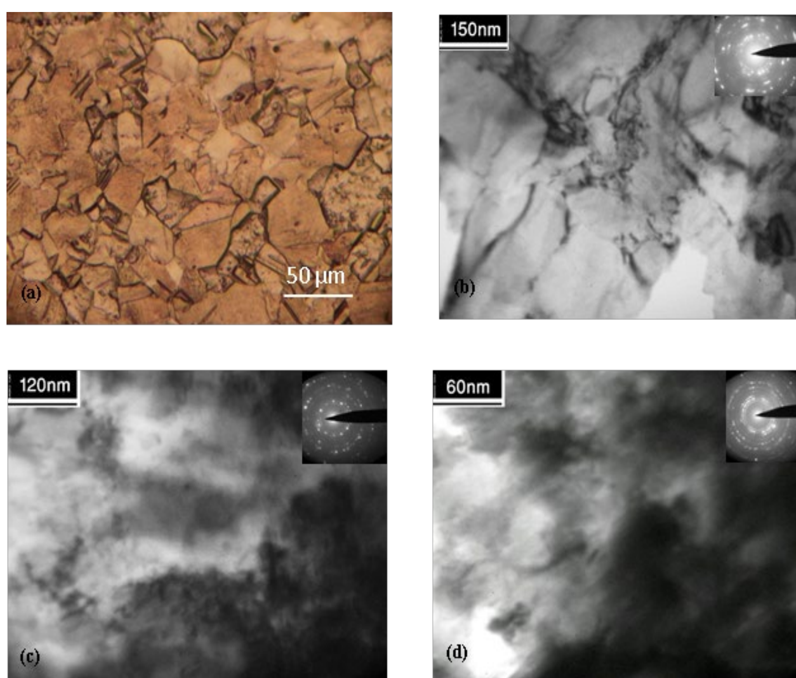

Fig. 3. (a) Annealed pure Cu optical micrograph, and (b-d) TEM micrographs and corresponding SAD patterns of 3, 5 and 7 cycles ARBed pure Cu specimens [96]. (With permission from Ref. [96]; License Number: 4707920802943, License date: Nov 14, 2019)

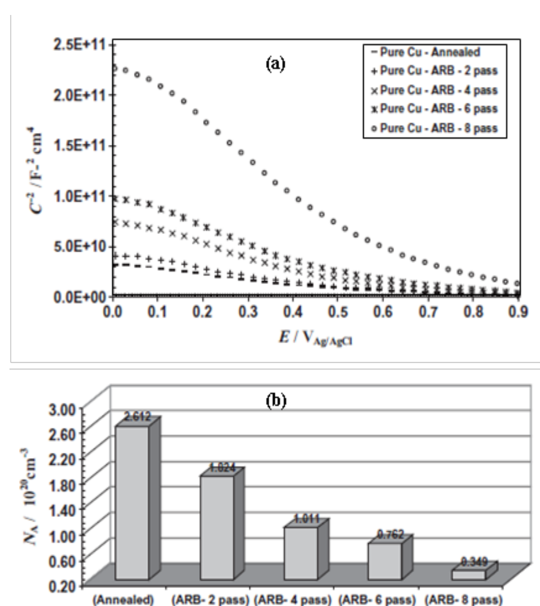

Fig. 4. (a) M–S plots and (b) variations in the N_A of pure Cu samples (Annealed and produced by ARB) in 0.01 M borax solution [12]. (With permission from Ref. [12]; License Number: 4707910404770, License date: Nov 14, 2019)

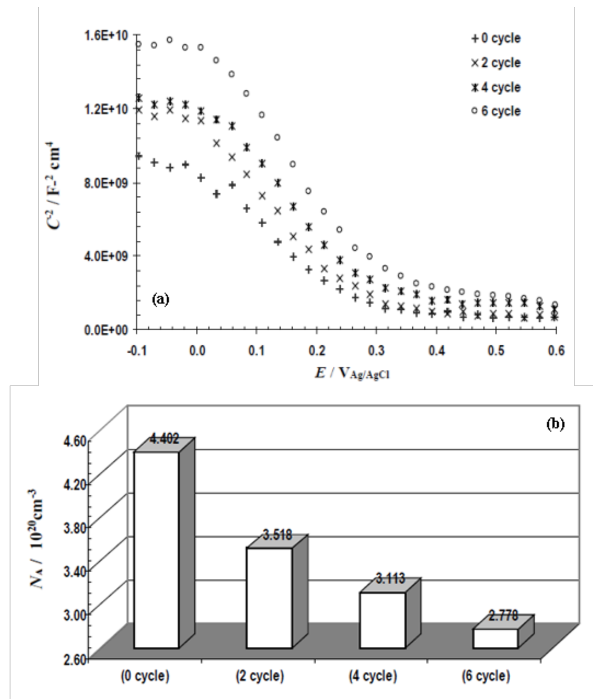

Fig. 5. (a) M–S plots and (b) variations in the N_A of pure Cu samples (Annealed and produced by ARB) in 0.01 M KOH solution [14]

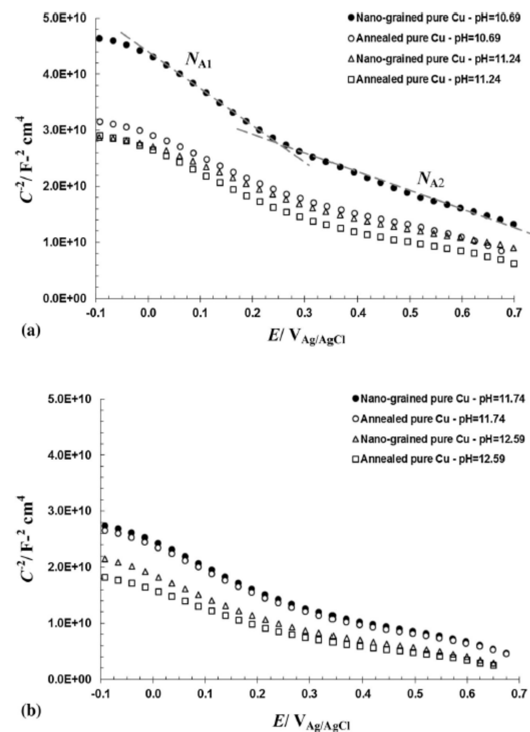

Fig. 6. M–S plots of annealed and NG pure Cu in phosphate buffer solutions: (a) pH=10.69 and 11.24, and (b) pH= 11.74 and 12.59 [17]. (With permission from Ref. [17]; License Number: 4710141135045, License date: Nov 15, 2019)

The plots of M–S for nano-grained (NG) and annealed pure Copper specimens in electrolytes of phosphate buffer (Fig. 6(a) and (b) [17]) show that the capacitances obviously declined by grain refinement. Table 3 indicates the obtained acceptor densities (N_{A1} and N_{A2}) of annealed and NG pure Cu specimens in solutions of phosphate buffer. Based on Table 3, acceptor densities declined in all electrolytes by the grain refinement procedure. The obtained acceptor densities are in the order of 10^{20} cm^{-3} that are similar to those of published amounts in the literature [10–12,14]. The existence of two acceptor densities can be ascribed to the distinct states of copper vacancies. The capacitance response is handled by the electronic structure of Cu^{1+} vacancies in the potentials lower than 0.25 $V_{Ag/AgCl}$. However, the capacitance response is controlled using the electronic structure of Cu^{2+} vacancies for potentials that are higher than 0.25 $V_{Ag/AgCl}$. Moreover, it is seen that the passive layer capacitance augmented when the pH increased. This rise in the passive layer capacitance is pointing to decline in the passivity of pure Copper and higher dissolution in solutions of phosphate buffer [17].

Table 3. Calculated acceptor densities (N_{A1} and N_{A2}) of annealed and nano-grained pure Cu in phosphate buffer solutions [17]. (With permission from Ref. [17]; License Number: 4710141135045, License date: Nov 15, 2019, Elsevier)

	N_{A1}/ $10^{20}cm^{-3}$		N_{A2}/ $10^{20}cm^{-3}$	
	Annealed pure copper	**Nano-grained pure copper**	**Annealed pure copper**	**Nano-grained pure copper**
pH=10.69	3.122	2.087	5.345	3.618
pH=11.24	3.236	2.914	5.567	3.954
pH=11.74	3.294	3.015	5.604	4.011
pH=12.59	4.323	3.733	5.903	4.681

Fig. 7(a) and (b) demonstrate the M–S plots of CG and NG pure Cu specimens after applying a different number of cyclic potentiodynamic passivation (CPP) treatment in 0.01 M borax [20]. As can be seen, the slope of M–S plots rises for both NG and CG pure Copper specimens when there is an increase in number of CPP cycles. It is clear that the passive film has a lower acceptor concentration after 100 cycles of CPP. The amounts of the N_A for both NG and CG pure Cu specimens were illustrated in Fig. 7(c) [20]. Based on Fig. 7(c), in the equal number of cycles, the N_A is fewer than that of for NG specimen. The N_A is the number of cation vacancies. Indeed, declining the number of cation vacancies in the passive layer augments the stability of passive layer and leads to an improved protection of metal. In the other words, rising the number of the CPP cycles in addition to the grain refinement, have

resulted in a decrease in concentration of defects within the passive film, ergo passive film obtains a better protective behavior. So, CPP has resulted in production of a less defective and thicker passive layer [20].

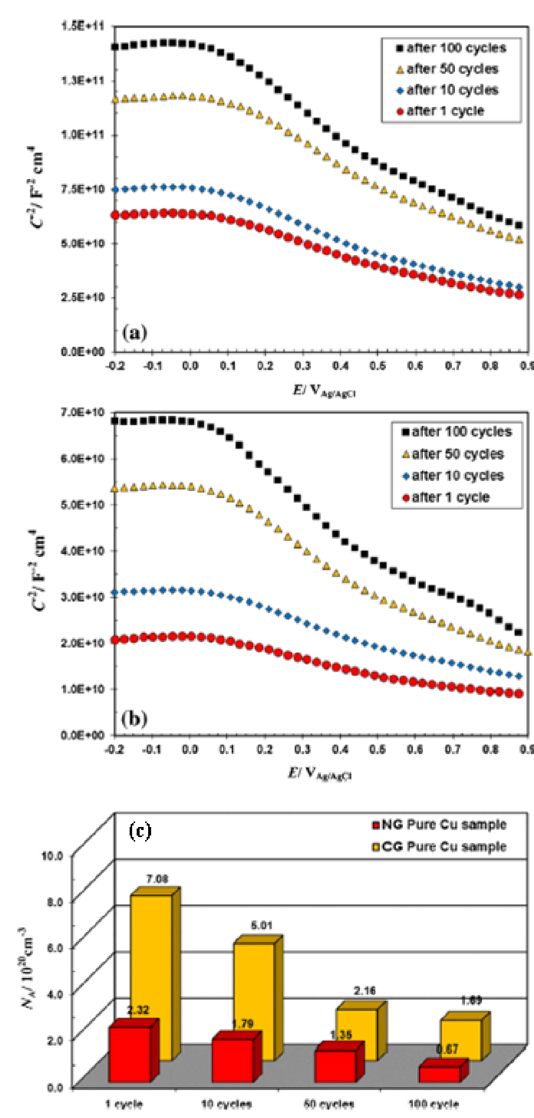

Fig. 7. (a, b) M–S plots and (c) variations in the N_A of NG and CG pure Cu specimens after different cycles in 0.01 M borax [20]. (With permission from Ref. [20]; License Number: 4707911081591, License date: Nov 14, 2019)

Fig. 8 shows the plots of M–S for the passive layers that were produced on NG and annealed pure copper specimens in solution of 0.01 M KOH by adding NaCl and without its addition [21]. All plots possess a near-linear area (except for an ARB processed specimen immersing in 0.01 M KOH+0.10 M NaCl). The seen negative slope in these plots infers that the produced passive layers on NG and annealed pure copper specimens have p-type semiconducting behavior where the vacancies of cation prevail. According to Fig. 8, C^{-2} declines obviously by

increasing the chloride ions concentration. Remarkably, C^{-2} rises because of grain refinement at each concentration of chloride ions. Table 4 shows the N_A of the passive layers that were formed on NG and annealed pure Copper specimens in solution of 0.01 M KOH with adding NaCl and without its addition. These high amounts of the N_A are ascribed to high densities of cation vacancies which are mainly placed near layer interface of passive/metal. Clearly, N_A rises by augmenting concentration of chloride ions. More significantly, passive layer of ARB processed specimen possesses lower levels of cation vacancies in any concentration; so, they are less defective [21]. Zhong et al. [95] evaluated the influence of grain size and chloride ion concentration on the semiconducting properties of copper using M–S analysis. They indicated that the N_A of the passivation layer on the surface of Copper declined in solution of borate buffer with different concentration of Cl^- by the declining the grain size [95].

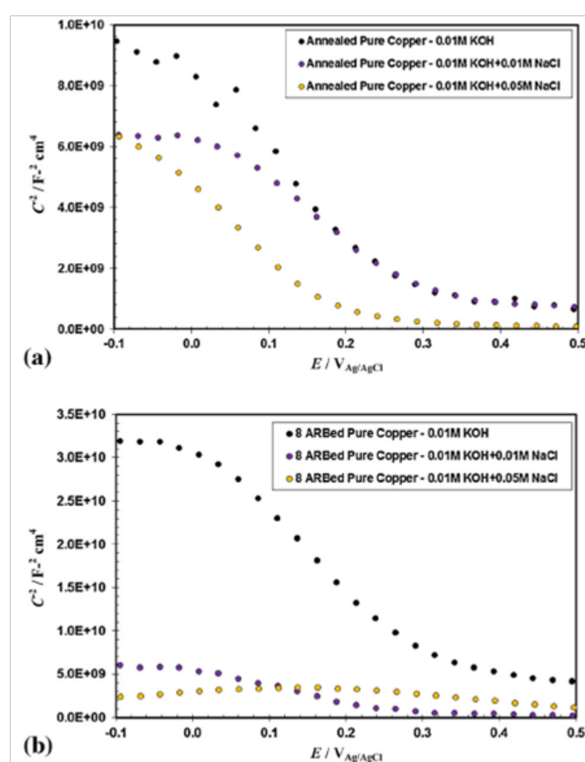

Fig. 8. M–S plots of passive film formed on annealed and NG pure Cu specimens in 0.01 M KOH solution with and without NaCl addition [21]. (With permission from Ref. [21]; License Number: 4710141195234, License date: Nov 15, 2019)

Indeed, adding chloride ions to the solution of alkaline rises the penetration of chloride ions to the passive layer by which more charge carriers are produced. Furthermore, Table 4 displays that grain refinement has reduced the Cl^- incorporation into the passive layer of ARB treated specimen [21].

Table 4. Variations of the acceptor densities of the passive films formed on annealed and nano-grained pure copper samples in 0.01 M KOH solution with and without NaCl addition [21]. (With permission from Ref. [21]; License Number: 4710141195234, License date: Nov 15, 2019, Elsevier)

	$N_A/10^{21}$ cm^{-3}	
	Annealed Pure Copper	**8 ARBed Pure Copper**
0.01 M KOH	0.440	0.124
0.01 M KOH+0.01 M NaCl	0.692	0.275
0.01 M KOH+0.05 M NaCl	0.701	-----

Fig. 9 indicates the variations and plots of M–S in the N_A of pure Cu specimens (cold worked and annealed specimens) in solution of 0.01 M NaOH [22].

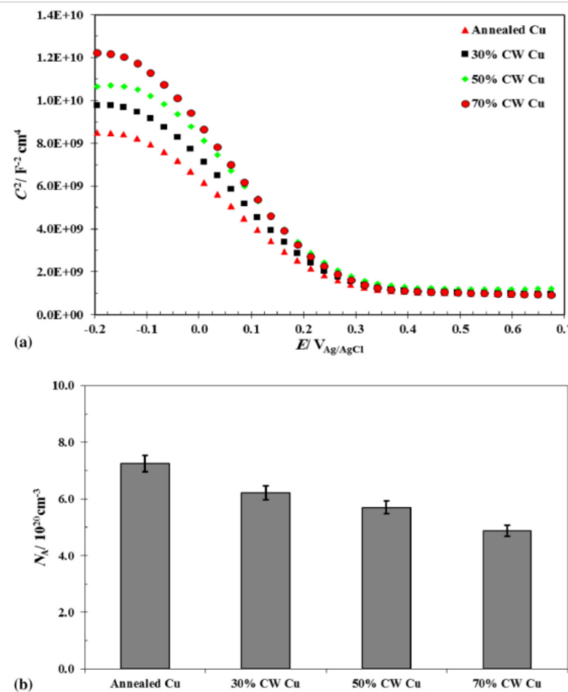

Fig. 9. (a) M–S plots and (b) variations in the N_A of pure copper specimens (annealed and cold worked samples) in 0.01 M NaOH solution [22]. (With permission from Ref. [22]; License Number: 4710141074857, License date: Nov 15, 2019)

According to this figure, linear relationship with negative slopes between C^{-2} and E shows that the produced passive layers on all Cu specimens are semiconductors of p-type.

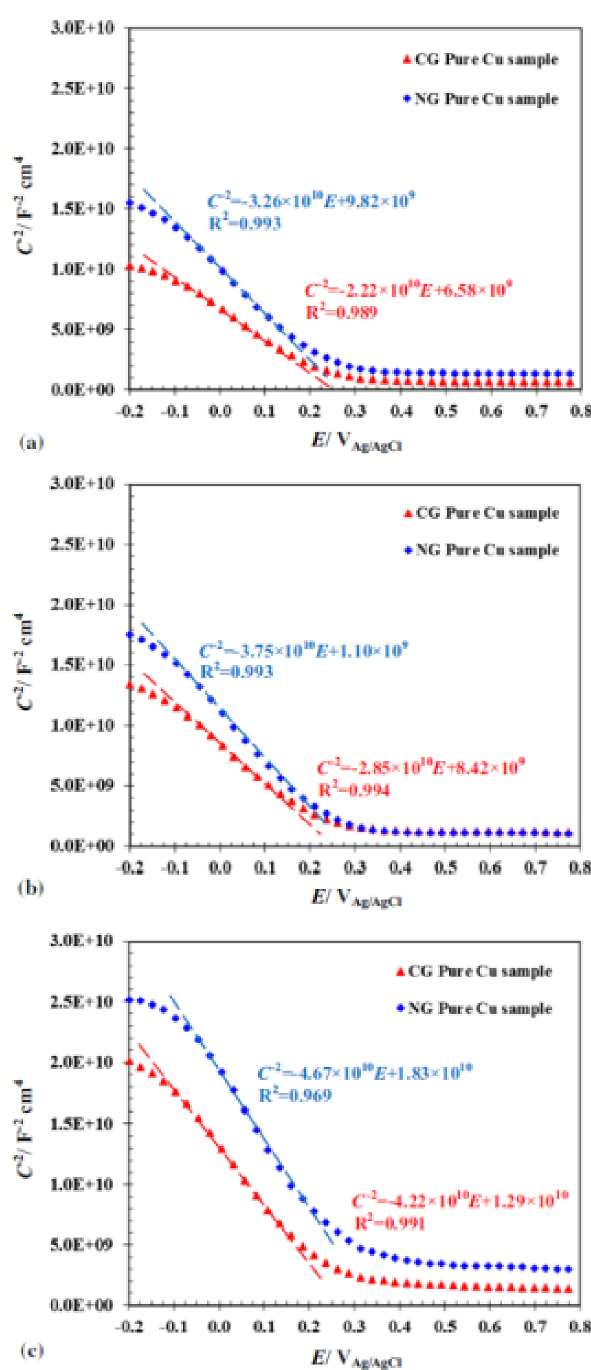

Fig. 10. Comparison of M–S plots of CG and NG pure copper samples after different numbers of CPP cycles: (a) 1, (b) 10, and (c) 50 cycles [24]. (With permission from Ref. [24]; License Number: 4710141014665, License date: Nov 15, 2019)

Fig. 9(b) shows the comparison of acceptor densities for the generated passive layers on the pure Cu specimens as a function of a decline in the thickness. In fact, density of acceptor for the produced passive layers helps passivation properties of pure Cu specimens. Considering the changes in dislocation density, microstrain and grain size, it can be considered that denser passive layer is produced by rising the percent reduction of thickness. However, higher

dislocation density, grain refinement and higher microstrain support surface of specimen to make a compact passive layer in electrolyte of 0.01 M NaOH [22].

Figs. 10 and 11 show the M–S plots and the variations in the N_A of CG and NG copper samples after different numbers of CPP cycles in 0.01 M KOH solution [24]. Based on Fig. 10, all specimens show a semiconducting behavior of p-type. According to the inverse relationship between the N_A and the slope of M–S plots, the steeper slope of NG specimens presents lower N_A for the similar amount of CPP cycles. Once again, the inference is that grain refinement enhances the copper passivation. The order of N_A in this procedure is 10^{20} cm^{-3} and this is comparable to the previous studies. Obviously, the N_A declines by employing more cycles of CPP, the implication being that compact stable passive layers are produced under the effect of this electrochemical process. This passive layer densification can be attributed to its less density of cation vacancies that are known as defects of lattice. To state the clear, the passive layer structure gets less defective after CPP process [24].

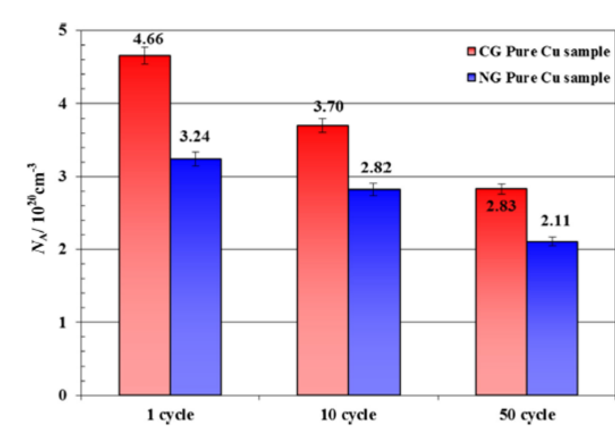

Fig. 11. Variations in the N_A of CG and NG pure copper samples in 0.01 M KOH solution [24]. (With permission from Ref. [24]; License Number: 4710141014665, License date: Nov 15, 2019)

The M–S curves and the variations in the N_A of the worked copper in terms of equal channel angular pressing (ECAP) passes in phosphate buffer solution are presented in Fig. 12 [25]. All plots possess a near-linear area, in which a linear relationship between C^{-2} and E sounds to be present. It is clear that capacitances rise by augmenting the passes of ECAP (Fig. 12(a)). Based on Fig. 12(b), the N_A declines with the number of ECAP passes. The orders of magnitude of the N_A are about 10^{20} cm^{-3} and are comparable to those published in other investigations [10,11].

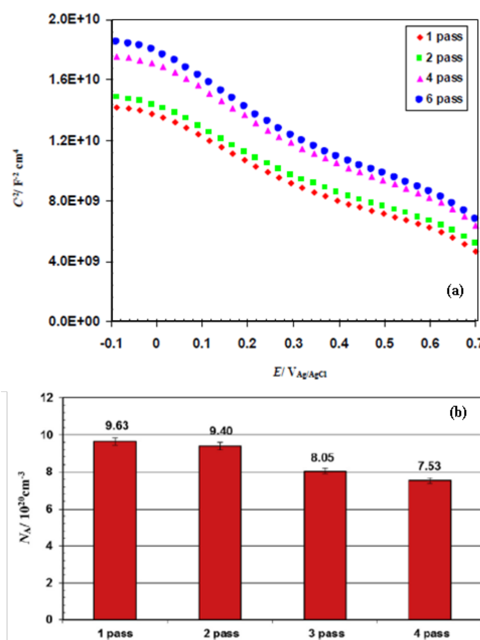

Fig. 12. (a) M–S plots and (b) variations in the N_A of ECAPed pure Cu samples in the phosphate buffer solution [25]. (With permission from Ref. [25]; License Number: 4710050057361, License date: Nov 15, 2019)

5. CONCLUSION

The effect of grain refinement on the semiconducting properties of pure Cu was investigated via M–S analysis. M–S results showed that the passive films act as semiconductor of p-type and grain refinement did not change the semiconductor behavior in alkaline electrolytes. The N_A values in the literature are normally from 10^{19} to 10^{21} cm^{-3}. Also, the precise amount depends on the used solution as the solution and microstructure. Providing dislocations, a high density of grain boundaries and other structural defects clearly resulted in grain refinement activates the surface of NG specimen where can exist as nucleation sites to form passive layer. On the other hand, it sounds grain refinement homogenizes the surface of NG specimen to an extent in which a compact passive layer is able to be produced. Unlike, a heterogeneous surface showing fairly few grains which are energetically distinct and fewer sites of nucleation exist in order to produce a passive layer For CG specimen.

REFERENCES

[1] V. Maurice, and P. Marcus, Electrochim. Acta 84 (2012) 129.
[2] V. Maurice, and P. Marcus, Solid State Mater. Sci. 22 (2018) 156.
[3] A. Fattah-alhosseini, A. Saatchi, M. A. Golozar, and K. Raeissi, Electrochim. Acta 54 (2009) 3645.

[4] A. Fattah-alhosseini, M. A. Golozar, A. Saatchi, and K. Raeissi, Corros. Sci. 52 (2010) 205.
[5] A. Fattah-alhosseini, F. Soltani, F. Shirsalimi, B. Ezadi, and N. Attarzadeh, Corros. Sci. 53 (2011) 3186.
[6] A. Fattah-alhosseini, Arab. J. Chem. 9 (2016) S1342.
[7] A. Veluchamy, D. Sherwood, B. Emmanuel, and I. S. Cole, J. Electroanal. Chem. 785 (2017) 196.
[8] N. E. Hakiki, Corros. Sci. 53 (2011) 2688.
[9] D. D. Macdonald, Pure Appl. Chem. 71 (1999) 951.
[10] A. Fattah-alhosseini, and S. Alizad, Anal. Bioanal. Electrochem. 7 (2015) 415.
[11] A. Fattah-alhosseini, M. K. Keshavarz, A. Masomi, and S. Marianaji, Egypt. J. Pet. 24 (2015) 405.
[12] A. Fattah-alhosseini, and O. Imantalab, J. Alloys Compd. 632 (2015) 48.
[13] O. Imantalab, and A. Fattah-alhosseini, J. Mater. Eng. Perform. 24 (2015) 2579.
[14] O. Imantalab, and A. Fattah-alhosseini, Anal. Bioanal. Electrochem. 7 (2015) 210.
[15] M. Pourbaix, Atlas of Electrochemical Equilibria in Aqueous Solutions Bokk, National Association of Corrosion; 2nd ed., Houston (1974).
[16] A. Fattah-alhosseini, A. H. Taheri, and M. K. Keshavarz, Trans. Indian Inst. Met. 69 (2016) 1423.
[17] O. Imantalab, A. Fattah-alhosseini, M. K. Keshavarz, and Y. Mazaheri, J. Mater. Eng. Perform. 25 (2016) 697.
[18] A. Fattah-alhosseini, and O. Imantalab, Metall. Mater. Trans. A 47 (2016) 572.
[19] O. Imantalab, A. Fattah-Alhosseini, Y. Mazaheri, and M. K. Keshavarz, Metall. Mater. Trans. A 47 (2016) 3684.
[20] A. Fattah-alhosseini, O. Imantalab, and F. R. Attarzadeh, Metall. Mater. Trans. B 47 (2016) 2761.
[21] A. Fattah-Alhosseini, O. Imantalab, and F. R. Attarzadeh, J. Mater. Eng. Perform. 25 (2016) 4478.
[22] A. Fattah-Alhosseini, M. Naseri, O. Imantalab, D. Gholami, and M. Haghshenas, J. Mater. Eng. Perform. 25 (2016) 4741.
[23] A. Fattah-alhosseini, and O. Imantalab, Anal. Bioanal. Electrochem. 8 (2016) 862.
[24] A. Fattah-alhosseini, O. Imantalab, F. R. Attarzadeh, and N. Attarzadeh, J. Mater. Eng. Perform. 26 (2017) 1634.
[25] D. Gholami, O. Imantalab, M. Naseri, S. Vafaeian, and A. Fattah-alhosseini, J. Alloy. Compd. 723 (2017) 856.
[26] M. Naseri, D. Gholami, O. Imantalab, F. R. Attarzadeh, and A. Fattah-Alhosseini, Mater. Res. Express. 5 (2018) 76504.
[27] A. Fattah-alhosseini, O. Ansari, Gh. Imantalab, Anal. Bioanal. Electrochem. 10 (2018)

805.
[28] A. Fattah-alhosseini, M. Naseri, S. O. Gashti, S. Vafaeian, and M. K. Keshavarz, Corros. Sci. 131 (2018) 81.
[29] A. Fattah-alhosseini, M. Naseri, S. O. Gashti, S. Vafaeian, and M. K. Keshavarz, J. Mater. Eng. Perform. 27 (2018) 3401.
[30] A. Fattah-Alhosseini, Z. Masomi, and M. Mirzaei, Anal. Bioanal. Electrochem. 6 (2014) 646.
[31] A. Fattah-alhosseini, Arab. J. Sci. Eng. 40 (2015) 63.
[32] A. Fattah-alhosseini, A. Jalali, and S. Felegari, Arab. J. Sci. Eng. 40 (2015) 2985.
[33] A. Fattah-Alhosseini, H. Aghamohammadi, and A. B. Safa, Anal. Bioanal. Electrochem. 7 (2015) 728.
[34] A. Fattah-Alhosseini, A. Khodabandeloie, and M. Bahiraee, J. Mater. Environ. Sci. 7 (2016) 1128.
[35] A. Fattah-Alhosseini, N. Rohani, and F. Khodaei, Anal. Bioanal. Electrochem. 9 (2017) 174.
[36] S. O. Gashti, and A. Fattah-Alhosseini, Anal. Bioanal. Electrochem. 6 (2014) 535.
[37] S. O. Gashti, A. Fattah-alhosseini, and Y. Mazaheri, Acta Metall. Sin. English Lett. 29 (2016) 629.
[38] S. O. Gashti, A. Fattah-alhosseini, Y. Mazaheri, M. K. Keshavarz, and E. J. Manuf. Process. 22 (2016) 269.
[39] S. O. Gashti, A. Fattah-alhosseini, Y. Mazaheri, and M. K. Keshavarz, J. Alloy. Compd. 688 (2016) 44.
[40] A. Fattah-Alhosseini, F. R. Attarzadeh, and M. Vakili-Azghandi, Metall. Mater. Trans. A. 48 (2017) 403.
[41] A. Fattah-alhosseini, M. Vakili-Azghandi, and M. Haghshenas, Int. J. Adv. Manuf. Technol. 90 (2017) 991.
[42] G. Ansari, and A. Fattah-alhosseini, Mater. Sci. Eng. C 75 (2017) 64.
[43] A. Fattah-alhosseini, A. R. Ansari, Y. Mazaheri, and M. K. Keshavarz, Mater. Sci. Eng. C 71 (2017) 771.
[44] A. Fattah-alhosseini, H. Elmkhah, and F. R. Attarzadeh, J. Mater. Eng. Perform. 26 (2017) 1792.
[45] F. R. Attarzadeh, H. Elmkhah, and A. Fattah-Alhosseini, Metall. Mater. Trans. B 48 (2017) 227.
[46] A. Fattah-alhosseini, M. Vakili-Azghandi, M. Sheikhi, and M. K. Keshavarz, J. Alloy. Compd. 704 (2017) 499.
[47] A. Ebrahimi, H. Esfahani, A. Fattah-alhosseini, and O. Imantalab, J. Alloys Compd. 765 (2018) 826.
[48] A. Ebrahimi, H. Esfahani, A. Fattah-alhosseini, and O. Imantalab, J. Mater. Eng. Perform.

28 (2019) 1456.
[49] A. Fattah-alhosseini, O. Imantalab, and G. Ansari, Mater. Sci. Eng. C 71 (2017) 827.
[50] A. Fattah-alhosseini, and S. Sharifi, Anal. Bioanal. Electrochem. 9 (2017) 862.
[51] F. R. Attarzadeh, N. Attarzadeh, S. Vafaeian, and A. Fattah-alhosseini, J. Mater. Eng. Perform. 25 (2016) 4199.
[52] A. Fattah-alhosseini, F. R. Attarzadeh, S. Vafaeian, M. Haghshenas, and M. K. Keshavarz, Met. Hard. Mater. 64 (2017) 168.
[53] A. Fattah-alhosseini, and M. Pourmahmoud, J. Mater. Eng. Perform. 27 (2018) 116.
[54] A. Fattah-alhosseini, H. Elmkhah, G. Ansari, F. Attarzadeh, and O. Imantalab, J. Alloy. Compd. 739 (2018) 918.
[55] A. Fattah-alhosseini, H. Elmkhah, K. Babaei, O. Imantalab, H. R. Ghomi, and M. K. Keshavarz, Mater. Res. Express. 5 (2018) 106401.
[56] A. Fattah-alhosseini, M. Roknian, and K. Babaei, Mater. Res. Express. 5 (2018) 116514.
[57] A. Fattah-alhosseini, S. Vafaeian, A. R. Ansari, and M. Khanmohammadi, Anal. Bioanal. Electrochem. 9 (2017) 660.
[58] A. Fattah-alhosseini, and M. Sabaghi Joni, J. Magnes. Alloy. 2 (2014) 175.
[59] A. Fattah-alhosseini, and M. Sabaghi Joni, J. Magnes. Alloy. 2 (2014) 305.
[60] A. Fattah-alhosseini, and M. S. Joni, J. Alloys Compd. 646 (2015) 685.
[61] A. Fattah-alhosseini, and M. S. Joni, Int. J. Mater. Res. 106 (2015) 282.
[62] M. J. M. Sabaghi Joni, and A. Fattah-alhosseini, Anal. Bioanal. Electrochem. 11 (2019) 448.
[63] A. Fattah-alhosseini, and H. Asgari, Arab. J. Sci. Eng. 41 (2016) 169.
[64] A. Fattah-alhosseini, and H. Asgari, J. Mater. Eng. Perform. 27 (2018) 3248.
[65] D. S. Kong, S. H. Chen, C. Wang, and W. Yang, Corros. Sci. 45 (2003) 747.
[66] A. Fattah-alhosseini, and M. Mirshekari, Trans. Indian Inst. Met. 68 (2015) 851.
[67] A. Fattah-alhosseini, and N. Attarzadeh, Anal. Bioanal. Electrochem. 7 (2015) 254.
[68] P. Mohamadian Samim, and A. Fattah-alhosseini, Anal. Bioanal. Electrochem. 8 (2016) 644.
[69] G. A. Zhang, Y. F. Cheng, Electrochim. Acta 55 (2009) 316.
[70] D. G. Li, Y. R. Feng, Z. Q. Bai, J. W. Zhu, and M. S. Zheng, Appl. Surf. Sci. 254 (2008) 2837.
[71] S. Ningshen, U. Kamachi Mudali, V. K. Mittal, and H. S. Khatak, Corros. Sci. 49 (2007) 481.
[72] A. Fattah-alhosseini, and S. Vafaeian, Egypt. J. Pet. 24 (2015) 333.
[73] A. Fattah-alhosseini, and S. Vafaeian, J. Alloys Compd. 639 (2015) 301.
[74] A. Fattah-alhosseini, and S. Vafaeian, J. Mater. Res. Technol. 4 (2015) 423.
[75] A. Fattah-alhosseini, and S. Vafaeian, Appl. Surf. Sci. 360 (2016) 921.
[76] S. Vafaeian, A. Fattah-alhosseini, M. K. Keshavarz, and Y. Mazaheri, J. Alloy. Compd.

677 (2016) 42.

[77] P. Mohamadian Samim, and A. Fattah-alhosseini, Anal. Bioanal. Electrochem. 8 (2016) 717.

[78] S. Vafaeian, A. Fattah-alhosseini, M. K. Keshavarz, and Y. Mazaheri, J. Mater. Eng. Perform. 26 (2017) 676.

[79] F. Qods, S. Maryanaji, and A. Fattah-alhosseini, Anal. Bioanal. Electrochem. 10 (2018) 161.

[80] D. D. MacDonald, Electrochim. Acta 56 (2011) 1761.

[81] Z. Lu, and D. D. Macdonald, Electrochim. Acta 53 (2008) 7696.

[82] D. D. Macdonald, J. Electrochem. Soc. 153 (2006) B213.

[83] D. D. Macdonald, J. Nucl. Mater. 379 (2008) 24.

[84] A. Fattah-alhosseini, and O. Imantalab, Anal. Bioanal. Electrochem. 8 (2016) 862.

[85] A. Fattah-alhosseini, A. R. Ansari, Y. Mazaheri, and M. Karimi, J. Mater. Eng. Perform. 26 (2017) 611.

[86] R. Khatami, A. Fattah-alhosseini, and M. K. Keshavarz, J. Alloys Compd. 708 (2017) 316.

[87] M. K. Keshavarz, and A. Fattah-alhosseini, Arab. J. Chem. (2018) doi:10.1016/j.arabjc.2018.01.021.

[88] C. Wang, J. Dong, W. Ke, and N. Chen, Jinshu Xuebao/Acta Metall. Sin. 47 (2011) 354.

[89] Y. Ling, M. L. Taylor, S. Sharifiasl, and D. D. Macdonald, ECS Trans. 50 (2013) 53.

[90] Q.J. Wang, J. Dong, W. Ke, and N. Chen, Corros. Eng. Sci. Technol. 52 (2015) 188.

[91] D. Kong, C. Dong, K. Xiao, and X. Li, Trans. Nonferrous Met. Soc. China 27 (2017) 1431.

[92] D. Kong, C. Dong, A. Xu, C. He, and X. Li, Corros. Eng. Sci. Technol. 52 (2017) 188.

[93] D. Kong, C. Dong, M. Zhao, X. Ni, C. Man, and X. Li, Corros. Eng. Sci. Technol. 53 (2018) 122.

[94] Q. J. Wang, M. S. Zheng, and J. W. Zhu, Thin Solid Films. 517 (2009) 1995.

[95] Q. J. Zhong, L. Bin Yu, Y. Xiao, Y. Wang, Q. Y. Zhou, and Q. D. Zhong, Adv. Mater. Res. 785–786 (2013) 928.

[96] A. Fattah-alhosseini, O. Imantalab, Y. Mazaheri, and M. K. Keshavarz, Mater. Sci. Eng. A 650 (2016) 8.

[97] Arash Fattah-alhosseini, M. Naseri, and K. Babaei, Anal. Bioanal. Electrochem. 11 (2019) 1353.

Copyright © 2020 by CEE (Center of Excellence in Electrochemistry)

ANALYTICAL & BIOANALYTICAL ELECTROCHEMISTRY (http://www.abechem.com)

Reproduction is permitted for noncommercial purposes.